

## **Supplementary materials for**

### **Seasonal variation of black carbon over the South China Sea and in various continental locations in South China**

Dui Wu<sup>1</sup>, Cheng Wu<sup>2</sup>, Biting Liao<sup>1</sup>, Fei Li<sup>1</sup>, Haobo Tan<sup>1</sup>, Tao Deng<sup>1</sup>, Haiyan Li<sup>1</sup>, Huizhong Chen<sup>1</sup>, Dehai Jiang<sup>1</sup>, Jian Zhen Yu<sup>2,3,4</sup>,

<sup>[1]</sup> Institute of Tropical and Marine Meteorology, CMA, Guangzhou 510080, China

<sup>[2]</sup> Division of Environment, Hong Kong University of Science and Technology, Clear Water Bay, Kowloon, Hong Kong, China

<sup>[3]</sup> Atmospheric Research Centre, Fok Ying Tung Graduate School, Hong Kong University of Science and Technology, Nansha, Guangzhou, China

<sup>[4]</sup> Department of Chemistry, Hong Kong University of Science and Technology, Clear Water Bay, Hong Kong, China

Correspondence to: Dui Wu ([wudui@grmc.gov.cn](mailto:wudui@grmc.gov.cn)), Jian Zhen Yu ([chjianyu@ust.hk](mailto:chjianyu@ust.hk))

#### **I. Supplementary figures**

There are a total of five supplementary figures. The  $\sigma_{\text{abs}}$  data in the dry and rainy seasons are summarized in Figure S1. Diurnal variations of  $\sigma_{\text{abs}}$  are shown in Figure S2. Figure S3 shows the weather chart for an example of tropical storm activity on May 17, 2008. Figure S4 shows the histogram of Angstrom Absorption Exponent (AAE) data at Yongxing (YX) in the dry season. AAE variations, along with  $\sigma_{\text{abs}}$  at multi wavelengths, are shown in Figure S5.

#### **II. Aethalometer data treatment**

The 7-channel Aethalometer (model AE31, Magee Scientific, USA) deployed in this study adopts one of the direct measurement techniques similar to the integrating plate method (Lin et al., 1973). Quartz fiber filter tape is used in Aethalometer for aerosol collection at a constant flow rate. Measurement of spectral light transmittance (370, 470, 520, 590, 660, 880, and 950 nm) of the filter tape is conducted at the end of each 5-min measurement cycle. The change of transmittance light intensities signal ( $I$ ) between each measurement cycle is recorded for attenuation (ATN) calculation, which is defined as follows:

$$ATN = 100 \cdot \ln \frac{I_0}{I} \quad (1)$$

where the  $I_0$  and  $I$  are the intensities of the transmission light through the filter without and with aerosol collected, respectively. When the attenuation of a sample spot on the filter reaches a certain threshold value (125 in this present study) at 370 nm after several cycles of measurements, the Aethalometer will automatically advance the filter tape to a new position for continual measurement. The light absorption coefficient of aerosol on filter can be derived from ATN via following equation:

$$\sigma_{ATN} = ATN \cdot \frac{A}{V} \quad (2)$$

Where  $\sigma_{ATN}$  is the light absorption coefficient of aerosol on filter,  $A$  is the spot area of aerosol deposit,  $V$  is the volume of air passing through the filter in each measurement cycle.

Data acquired from filter-based measurement such as Aethalometer needs carefully correction due to its inherent systemic error (Weingartner et al., 2003; Virkkula et al., 2007; Schmid et al., 2006; Arnott et al., 2005). Coen summarized three known artifacts (Coen et al., 2010), i.e., filter matrix effect, scattering effect and loading effect. The non-linear relationship between  $\sigma_{ATN}$  and  $\sigma_{abs}$  (the light absorption coefficient of suspended aerosol in ambient air) has become a challenge for Aethalometer, as a linear relationship is assumed by default in its output data. The correction algorithm proposed by Weingartner (Weingartner et al., 2003) was applied in this study to treat the 5-min measurement data:

$$\sigma_{abs} = \frac{\sigma_{ATN}}{C_{ref} \cdot R(ATN)} \quad (3)$$

where  $C_{ref}$  is the constant representing the correction for matrix effect,  $R(ATN)$  is an function of ATN to correct for the loading effect, which is shown in Eq. (3).

$$R(ATN) = \left( \frac{1}{f} - 1 \right) \frac{\ln(ATN\%) - \ln(10\%)}{\ln(50\%) - \ln(10\%)} + 1 \quad (4)$$

The underlying idea is to first correct all  $\sigma_{ATN}$  to  $\sigma_{10\%}$ , which then can be corrected into  $\sigma_{abs}$  values through the calibration factor  $C_{ref}$ .  $C_{ref} = 3.48$  was applied in this study and this value was obtained from the slope of the plot of  $\sigma_{ATN}$  by Aethalometer vs.  $\sigma_{abs}$  by PAS (Photo-Acoustic Spectrometer) during a comparison study in Pearl River Delta region (Wu et al., 2009). This value is higher but similar to those reported in literature: 2.13 by Weingartner (Weingartner et al., 2003) and 1.9 by Bodhaine (Bodhaine, 1995). The  $f$  value in Eq. (4) depends on aerosol types and their mixing state, which is determined through chamber studies (Weingartner et al., 2003). A previous study in the PRD found that soot particles are mainly externally mixed in this region (Cheng et al., 2006). Therefore, corresponding  $f$  values are chosen from Weingartner's study.

The following criteria were applied in data treatment to screen out the invalid data points: (1) AAE should be in the range of 0.5 to 6; (2) data must be available in all seven wavelengths

## References

- Arnott, W. P., Hamasha, K., Moosmuller, H., Sheridan, P. J., and Ogren, J. A.: Towards aerosol light-absorption measurements with a 7-wavelength Aethalometer: Evaluation with a photoacoustic instrument and 3-wavelength nephelometer, *Aerosol Sci Tech*, 39, 17-29, Doi 10.1080/027868290901972, 2005.
- Bodhaine, B. A.: Aerosol Absorption-Measurements at Barrow, Mauna-Loa and the South-Pole, *J Geophys Res-Atmos*, 100, 8967-8975, 1995.
- Cheng, Y. F., Eichler, H., Wiedensohler, A., Heintzenberg, J., Zhang, Y. H., Hu, M., Herrmann, H., Zeng, L. M., Liu, S., Gnauk, T., Brüggemann, E., and He, L. Y.: Mixing state of elemental carbon and non-light-absorbing aerosol components derived from in situ particle optical properties at Xinken in Pearl River Delta of China, *J Geophys Res-Atmos*, 111, D20204 Doi 10.1029/2005jd006929, 2006.
- Coen, M. C., Weingartner, E., Apituley, A., Ceburnis, D., Fierz-Schmidhauser, R., Flentje, H., Henzing, J. S., Jennings, S. G., Moerman, M., Petzold, A., Schmid, O., and Baltensperger, U.: Minimizing light absorption measurement artifacts of the Aethalometer: evaluation of five correction algorithms, *Atmos Meas Tech*, 3, 457-474, 2010.
- Lin, C.-I., Baker, M., and Charlson, R. J.: Absorption Coefficient of Atmospheric Aerosol: a Method for Measurement, *Appl. Opt.*, 12, 1356-1363, 1973.
- Schmid, O., Artaxo, P., Arnott, W. P., Chand, D., Gatti, L. V., Frank, G. P., Hoffer, A., Schnaiter, M., and Andreae, M. O.: Spectral light absorption by ambient aerosols influenced by biomass burning in the Amazon Basin. I: Comparison and field calibration of absorption measurement techniques, *Atmos Chem Phys*, 6, 3443-3462, 2006.
- Virkkula, A., Mäkelä, T., Hillamo, R., Yli-Tuomi, T., Hirsikko, A., Hameri, K., and Koponen, I. K.: A simple procedure for correcting loading effects of aethalometer data, *J Air Waste Manage*, 57, 1214-1222, 2007.
- Weingartner, E., Saathoff, H., Schnaiter, M., Streit, N., Bitnar, B., and Baltensperger, U.: Absorption of light by soot particles: determination of the absorption coefficient by means of aethalometers, *J Aerosol Sci*, 34, 1445-1463, Doi 10.1016/S0021-8502(03)00359-8, 2003.
- Wu, D., Mao, J. T., Deng, X. J., Tie, X. X., Zhang, Y. H., Zeng, L. M., Li, F., Tan, H. B., Bi, X. Y., Huang, X. Y., Chen, J., and Deng, T.: Black carbon aerosols and their radiative properties in the Pearl River Delta region, *Sci China Ser D*, 52, 1152-1163, DOI 10.1007/s11430-009-0115-y, 2009.

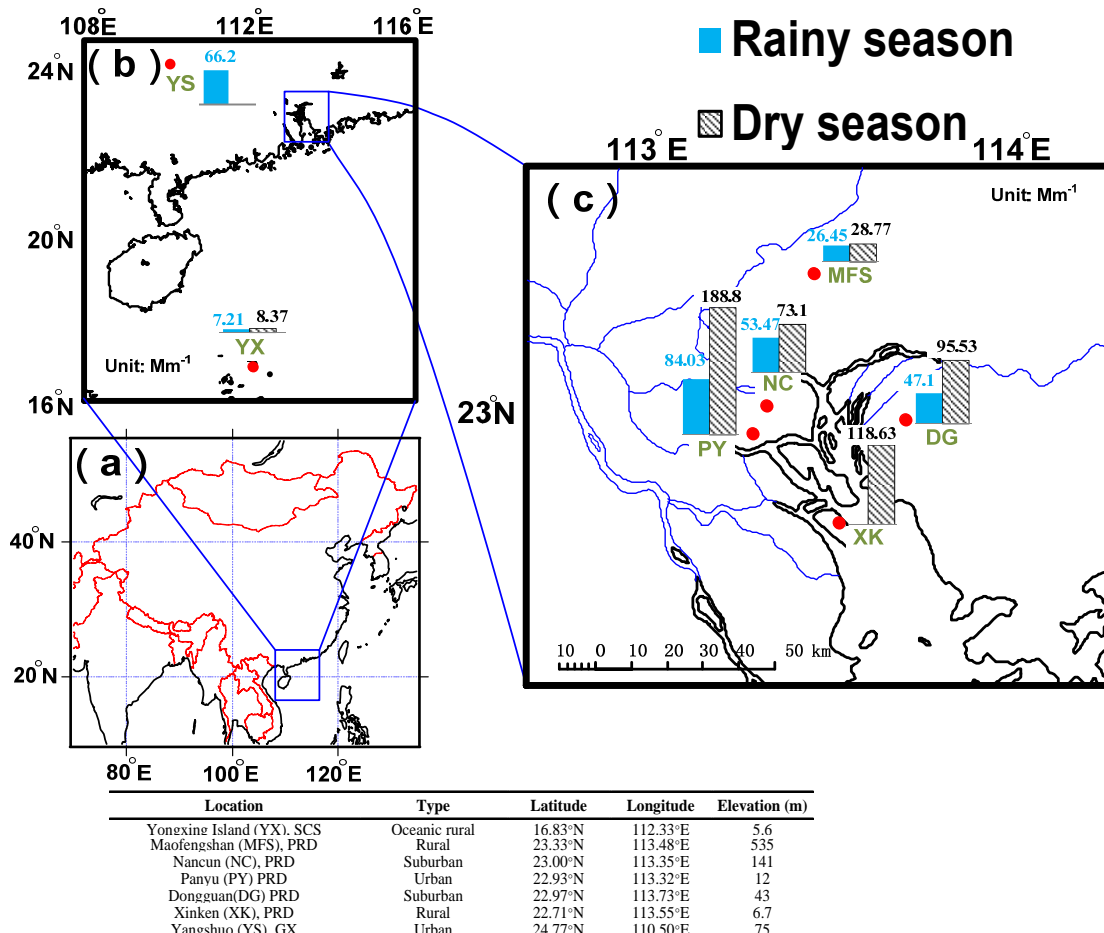


**Figure S1.** Average light absorption coefficients ( $\sigma_{abs}$ ) in  $\text{Mm}^{-1}$  during rainy and dry seasons across different sampling sites in column plots on the map (column plots in different maps are on the same scale). The enclosed table summarizes the characteristics of sampling sites in this study. (a) Location of the study region in China, (b) Location of two short-term sites: the oceanic site at Yongxing island (YX) and the urban site Yangshuo (YS). (c) Location of the long-term sites in PRD, including Maofengshan (MFS), Nancun (NC), Panyu, (PY), Dongguan (DG), Xinken(XK).

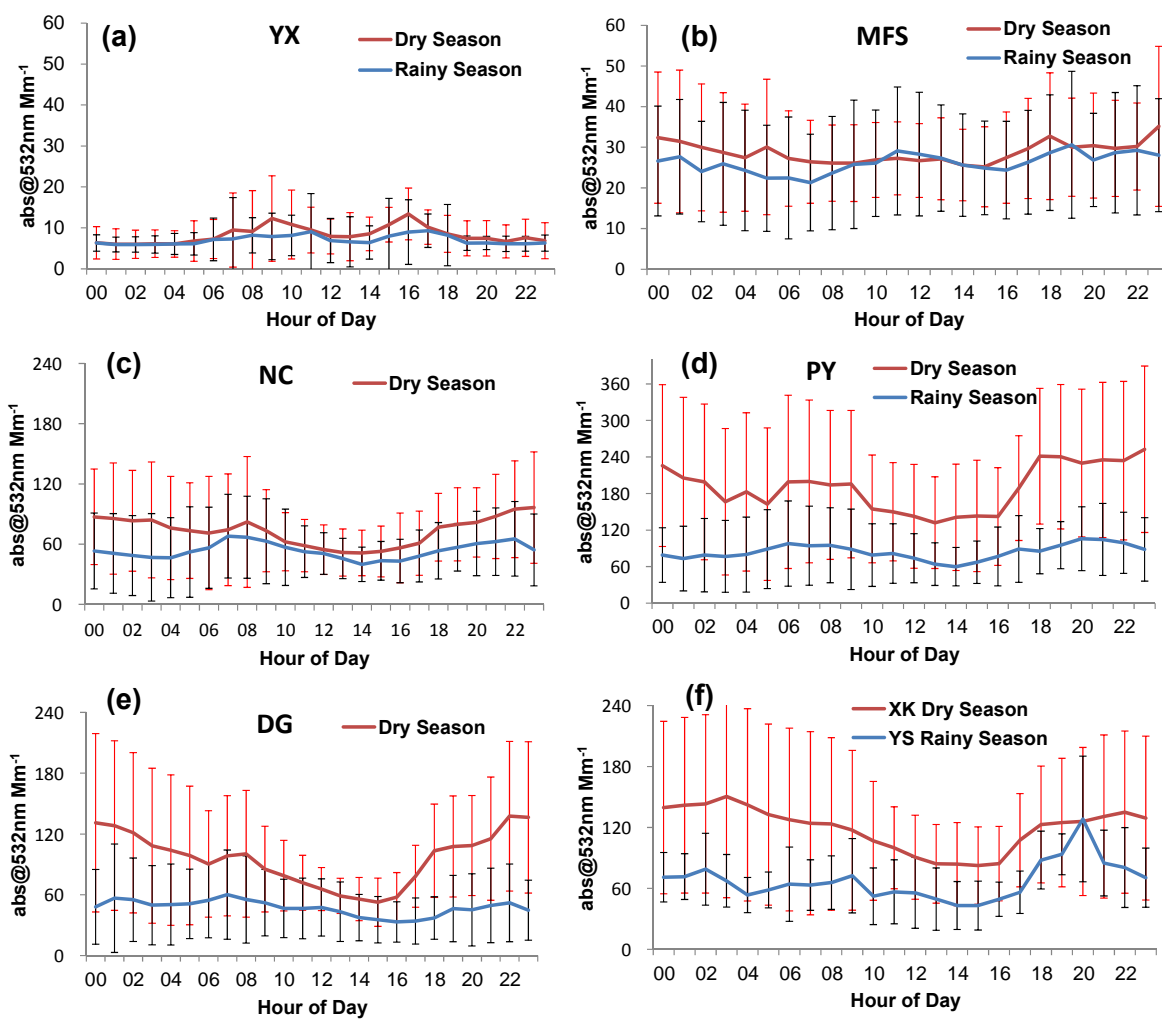


**Figure S2.** Diurnal variations of absorption coefficients at six monitoring sites in rainy and dry seasons. The sites are (a) Maofengshan (MFS), (b) Yongxing island (YX), (c) Nancun (NC), (d) Panyu (PY), (e) Dongguan (DG), and (f) Xinken (XK) in dry season and Yangshuo (YS) in rainy season.

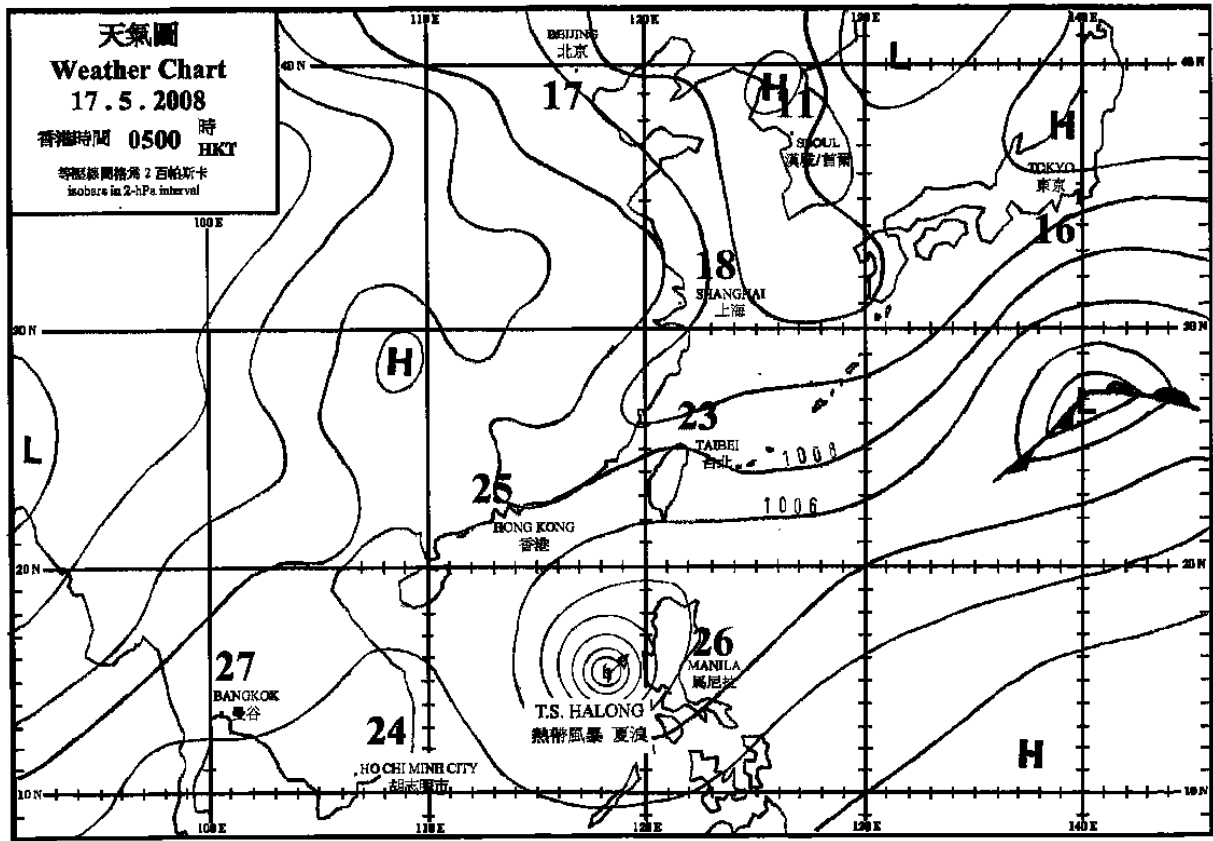


Figure S3. Tropical storm Halong over the South China Sea when approaching Philippines (17 May 2008 5:00)

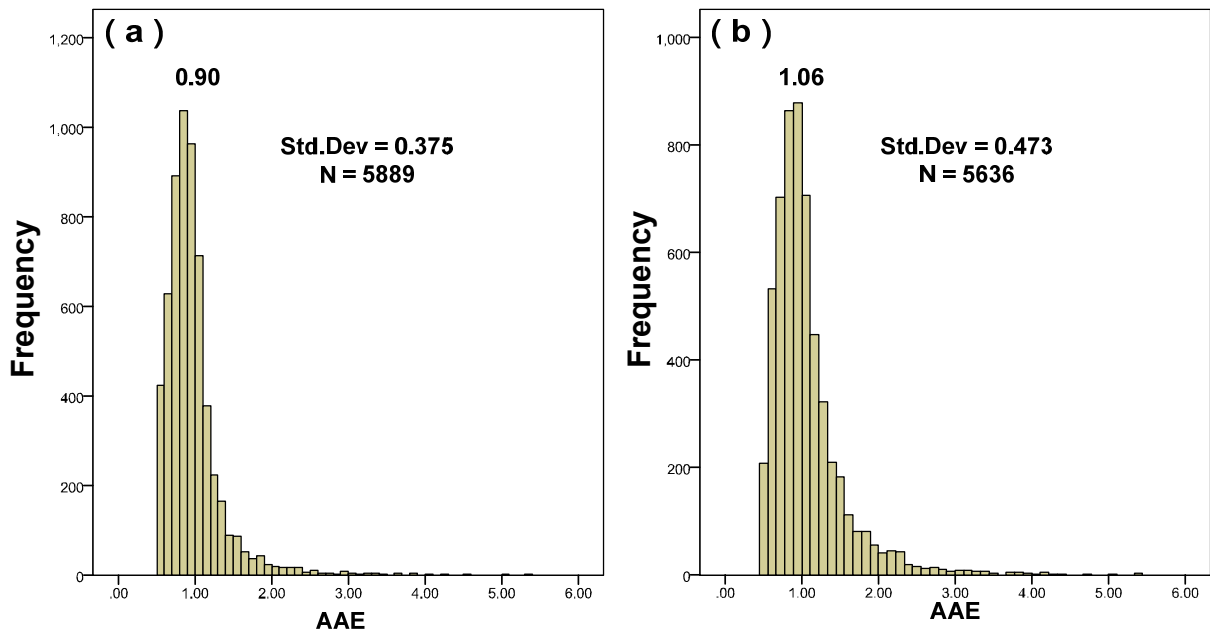
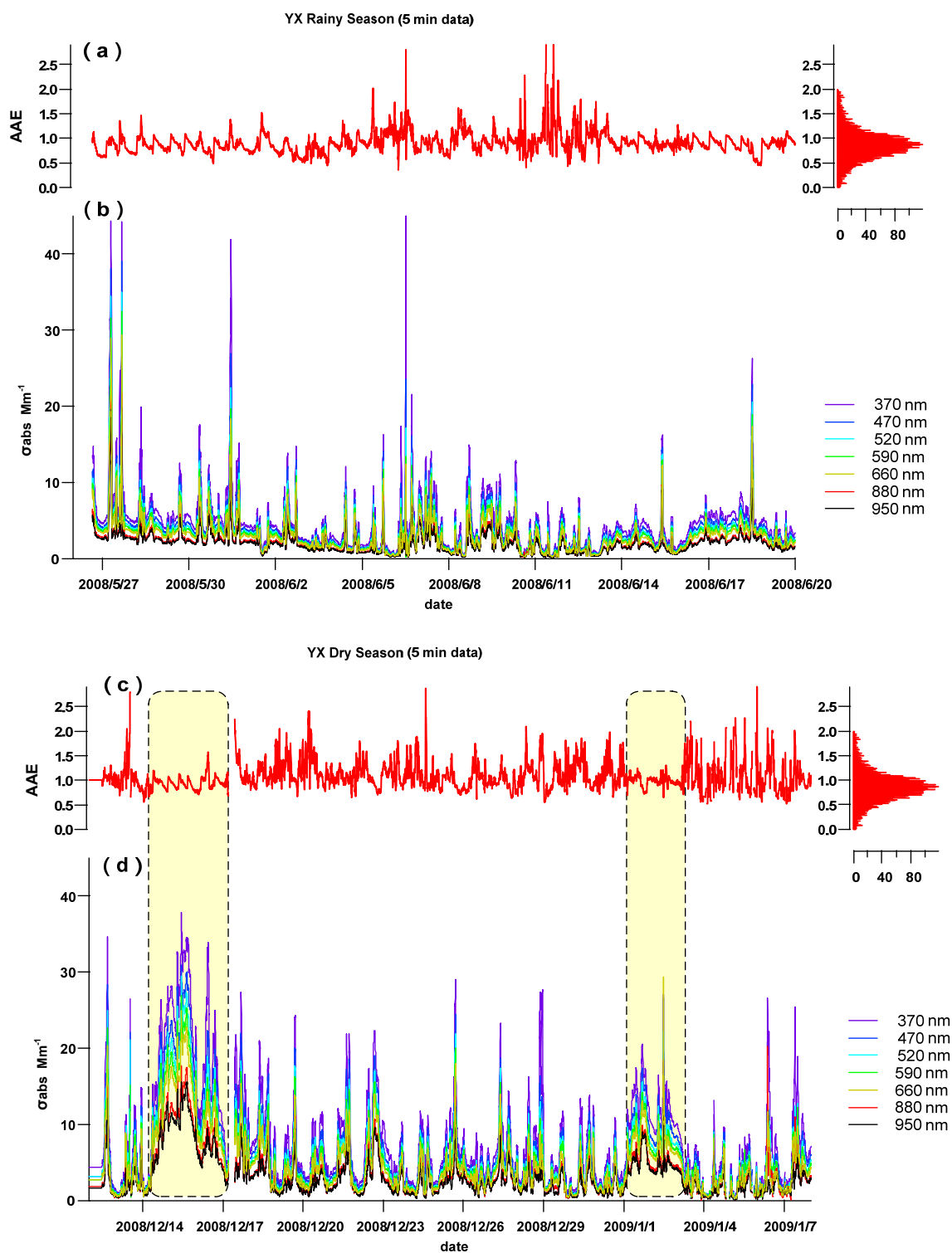


Figure S4. Distribution of Absorption Angstrom Exponent (AAE) values at YX in (a) Rainy season and (b) Dry season.



**Figure S5.** Time series variations (5 min data) of: **(a)** Absorption Angstrom Exponent (AAE) at YX during rainy season; **(b)**  $\sigma_{\text{abs}}$  at seven wavelengths at YX during rainy season; **(c)** AAE at YX during dry season; **(d)**  $\sigma_{\text{abs}}$  at seven wavelengths at YX during dry season. The highlighted areas mark two episodic events observed during dry season.